

D-A248 449



2

AD

TECHNICAL REPORT ARCCB-TR-92007

X-RAY DIFFRACTION STUDY OF RESIDUAL STRESSES IN METAL MATRIX COMPOSITE-JACKETED STEEL CYLINDERS SUBJECTED TO INTERNAL PRESSURE

S.L. LEE
M. DOXBECK
G. CAPSIMALIS



MARCH 1992



**US ARMY ARMAMENT RESEARCH,
DEVELOPMENT AND ENGINEERING CENTER
CLOSE COMBAT ARMAMENTS CENTER
BENÉ LABORATORIES
WATERVLIET, N.Y. 12189-4050**



APPROVED FOR PUBLIC RELEASE; DISTRIBUTION UNLIMITED

92-09196



92 4 09 051

DISCLAIMER

The findings in this report are not to be construed as an official Department of the Army position unless so designated by other authorized documents.

The use of trade name(s) and/or manufacturer(s) does not constitute an official indorsement or approval.

DESTRUCTION NOTICE

For classified documents, follow the procedures in DoD 5200.22-M, Industrial Security Manual, Section II-19 or DoD 5200.1-R, Information Security Program Regulation, Chapter IX.

For unclassified, limited documents, destroy by any method that will prevent disclosure of contents or reconstruction of the document.

For unclassified, unlimited documents, destroy when the report is no longer needed. Do not return it to the originator.

REPORT DOCUMENTATION PAGE

Form Approved
OMB No. 0704-0188

Public reporting burden for this collection of information is estimated to average 1 hour per response, including the time for reviewing instructions, searching existing data sources, gathering and maintaining the data needed, and completing and reviewing the collection of information. Send comments regarding this burden estimate or any other aspect of this collection of information, including suggestions for reducing this burden, to Washington Headquarters Services, Directorate for Information Operations and Reports, 1215 Jefferson Davis Highway, Suite 1204, Arlington, VA 22202-4302, and to the Office of Management and Budget, Paperwork Reduction Project (0704-0188), Washington, DC 20503.

1. AGENCY USE ONLY (Leave blank)		2. REPORT DATE March 1992	3. REPORT TYPE AND DATES COVERED Final	
4. TITLE AND SUBTITLE X-RAY DIFFRACTION STUDY OF RESIDUAL STRESSES IN METAL MATRIX COMPOSITE-JACKETED STEEL CYLINDERS SUBJECTED TO INTERNAL PRESSURE			5. FUNDING NUMBERS AMCMS No. 612623H2100 PRON No. 4A8GEV314A1A	
6. AUTHOR(S) S.L. Lee, M. Doxbeck, and G. Capsimalis				
7. PERFORMING ORGANIZATION NAME(S) AND ADDRESS(ES) U.S. Army ARDEC Benet Laboratories, SMCAR-CCB-TL Watervliet, NY 12189-4050			8. PERFORMING ORGANIZATION REPORT NUMBER ARCCB-TR-92007	
9. SPONSORING/MONITORING AGENCY NAME(S) AND ADDRESS(ES) U.S. Army ARDEC Close Combat Armaments Center Picatinny Arsenal, NJ 07806-5000			10. SPONSORING/MONITORING AGENCY REPORT NUMBER	
11. SUPPLEMENTARY NOTES Presented at the 4th International Conference of Non-Destructive Characterization of Materials, Annapolis, MD, June 1990 Published in the Proceedings of the Conference				
12a. DISTRIBUTION/AVAILABILITY STATEMENT Approved for public release; distribution unlimited			12b. DISTRIBUTION CODE	
13. ABSTRACT (Maximum 200 words) The study of aluminum/silicon carbide metal matrix composite (MMC)-jacketed steel structural components was made because of their light weight and high stiffness. Steel 'liner' cylinders were wrapped with MMC 'jackets' with an all-hoop layup and put through various degrees of hydraulic autofrettage and thermal soak. In this report, the results from our x-ray diffraction residual stress measurements on cylinders using a position-sensitive scintillation detection system are discussed. Our experimental results are compared with theoretical predictions from a model based on the elastic-plastic analysis of a thick-walled cylinder subjected to internal pressure. Interpretation of the interference effect caused by the MMC jacket on the steel liner is also discussed.				
14. SUBJECT TERMS Residual Stress, Pressure Vessel, Metal Matrix Composites, Autofrettage, Stress Distribution, Jacketed Steel Cylinder, Aluminum/Silicon Carbide, Thermal Relaxation			15. NUMBER OF PAGES 17	
			16. PRICE CODE	
17. SECURITY CLASSIFICATION OF REPORT UNCLASSIFIED	18. SECURITY CLASSIFICATION OF THIS PAGE UNCLASSIFIED	19. SECURITY CLASSIFICATION OF ABSTRACT UNCLASSIFIED	20. LIMITATION OF ABSTRACT UL	

TABLE OF CONTENTS

	<u>Page</u>
ACKNOWLEDGEMENTS	iii
INTRODUCTION	1
EXPERIMENTAL METHOD	2
CYLINDER PROCESSING HISTORY	3
SPECIMEN PREPARATION	5
CALIBRATION AND VERIFICATION PROCEDURE	6
EXPERIMENTAL RESULTS	6
THEORETICAL CONSIDERATION	9
DISCUSSION	11
REFERENCES	13

TABLES

I. COMPARISON OF MATERIAL PROPERTIES OF STEEL AND ALUMINUM/SILICON CARBIDE METAL MATRIX COMPOSITES	2
II. CYLINDER PROCESSING HISTORY	5

LIST OF ILLUSTRATIONS

1. Jacketed cylinder geometry	4
2. Four-point bend verification	6
3. The measured 3AE02 hoop residual stress distribution	7
4. The measured 3AE05 hoop residual stress distribution	7
5. The measured 3AA hoop residual stress distribution with a line superimposed showing the predicted stress distribution	7
6. The measured 3AN hoop residual stress distribution with a line superimposed showing the predicted stress distribution	7
7. $\sin^2\psi$ determination of stresses at the cylinder bore	8

8. $\text{Sin}^2\psi$ determination of stresses at the interface	8
9. Decomposition of composite/steel cylinder	9
10. Monoblock plastic deformation calculations with 3AA and 3AE02 hoop residual stress distributions superimposed	10

ACKNOWLEDGEMENTS

The authors wish to thank Peter Chen for the theoretical results, John Underwood for helpful discussions, Gary Cunningham for the compound cylinders and material constants, and Robert Messier and John Hoffman for preparing the rings.

Accession For	
NTIS GRA&I	<input checked="" type="checkbox"/>
DTIC TAB	<input type="checkbox"/>
Unannounced	<input type="checkbox"/>
Justification	
By	
Distribution/	
Availability Codes	
Dist	Avail and/or Special
A-1	

INTRODUCTION

Metal matrix composite (MMC)-jacketed steel cylinders have been designed and fabricated to obtain the same pressure containment as steel cylinders, but with much less weight. The manufacturing and testing of the MMC-jacketed cylinder program has been summarized in a Benet Laboratories technical report (ref 1). As indicated in Table I (ref 1), the steel has a density of 0.28 lb/in.³, and the MMC jacket (continuous silicon carbide wrapped in the hoop direction and sprayed with 6061 aluminum alloy matrix) has a density of 0.11 lb/in.³. The ultimate tensile strength (UTS) is 178 Ksi for the steel and 217 Ksi for the MMC. The MMC is used because of its light weight (2.6 times less than steel) and its comparable UTS.

In this report, our x-ray diffraction measurements of the residual stress using a position-sensitive scintillation detection (PSSD) system are presented. The cylinders were subjected to various pressure cycles and then autofrettaged and thermal soaked. The autofrettage process can induce favorable residual stress distribution in the cylinders and improve fatigue and fracture behavior. Because applied and residual stresses add algebraically, the autofrettage procedure has been applied to increase the elastic operating pressure of a system. However, cylinders subjected to heating can lose residual stress. In high temperature applications, a thermal soak process is applied to release some of the residual stress generated by autofrettage to obtain thermally-stable components. Our experimental results are compared with predictions from a model based on the elastic and plastic analyses of a thick-walled composite tube subjected to internal pressure. The effect of the MMC on the steel liner is discussed.

TABLE I. COMPARISON OF MATERIAL PROPERTIES OF STEEL AND ALUMINUM/SILICON CARBIDE METAL MATRIX COMPOSITES

Property	Steel	MMC
Weight density (lb/in. ³)	0.283	0.11
Ultimate tensile strength (Ksi) (MMC with hoop layup)	178	217
Yield strength (Ksi)	155	-
Young's modulus (Msi)- (MMC with hoop layup)		
E11	30	32
E22, E33		19
Poisson's ratio- (MMC with hoop layup)		
V12, V13	0.28	0.25
V21, V31		0.14
V23, V32		0.36

EXPERIMENTAL METHOD

A D-1000-A Denver X-Ray Instruments Model stress analyzer design was used based on a Ruud-Barrett PSSD. The instrumentation and experimental methods are described in References 2 and 3. The instrument utilizes a miniature x-ray tube that fits inside a cylinder with a 3.70-inch interior diameter. The operating principles for this detection system consist of converting incident x-rays into light through cadmium-zinc sulfide scintillation coating; transporting this light to a detector package through fiber optics bundles; amplifying the light intensity through an image intensifier; and converting it into an electronic signal through a 512-element reticon photodiode array. The instrument uses a chromium target tube and can exploit x-ray sources of 100 watts or less, thus providing a very short data collection time interval. The characteristic x-ray radiation from the chromium tube does not fluoresce any major alloys in steel.

The chromium K- α reflects from the 211 plane of the body-centered-cubic (BCC) carbon steel and the 211 plane of the BCC martensitic steel at $2\theta = 156.41$ degrees. The divergent x-ray beam was collimated by a square slit; the irradiated area at the specimen was approximately $(1/16)^2$ in.².

An IBM AT computer is connected to the system for data acquisition, control, storage, and analysis. The instrumentation allows both single-exposure and multiple-exposure ($\sin^2\psi$) methods of residual stress determination. In the single-exposure technique, residual stress is determined from two x-ray diffraction patterns obtained simultaneously in a single exposure. In the $\sin^2\psi$ technique, stress is determined from diffraction patterns obtained at multiple angles of inclination. The diffraction peaks are noise- and gain-corrected. Typical data collection time for a steel sample is 2 to 3 seconds. In addition, the software uses a number of algorithms to correct electronic and mechanical hardware fluctuations, x-ray focusing errors, and effects due to polarization and absorption. A parabolic fit taking 50 percent of the upper part of the diffraction peak is used to make the final peak determination.

In this report, stress distribution measurements were made in the steel liner using the single-exposure technique. The bore and interface stresses were further confirmed by $\sin^2\psi$ measurements. In the latter method, four β angles at 12, 20, 27, and 33 degrees, giving eight data points for the linear regression fit were used. The β angle is the angle between the specimen surface normal and the incident x-ray beam. In addition to the system software, SYMPHONY and FREELANCE software were used for data analysis and graphics.

CYLINDER PROCESSING HISTORY

The geometry of the jacketed cylinders is shown in Figure 1. The cylinders are ASTM A723 steel forging approximately one foot long, with a bore diameter of

4.5 inches, a steel liner thickness of 0.4 inch, and an MMC jacket thickness of 0.2 inch. This geometry gives a 2.25-inch steel liner inside radius, a 2.65-inch steel/MMC interface radius, and a 2.85-inch MMC outside radius. As a result, the steel liner has 64 percent of the total volume and 82 percent of the total weight, while the MMC has 36 percent of the total volume and 18 percent of the total weight. The total component weight savings of the compound cylinder compared to an all-steel cylinder is 22 percent. The liner was wrapped directly with the silicon carbide fibers in the circumferential direction, and the 6061 aluminum alloy matrix was applied by plasma spray. The monofilament reinforcing silicon carbide fibers were 0.0056 inch in diameter and occupied 47 percent of the total MMC volume. The steel cylinders were manufactured by Benet Laboratories, while the MMC wrapping was done by Textron Specialty Materials Division (Lowell, MA). Interlayers were plated on the liners consisting of 0.001 to 0.002 inch of nickel, silver, and aluminum/10 percent silver alloy. The purpose of the interlayers was to create a better bond and to reduce galvanic corrosion between the jacket and the liner.

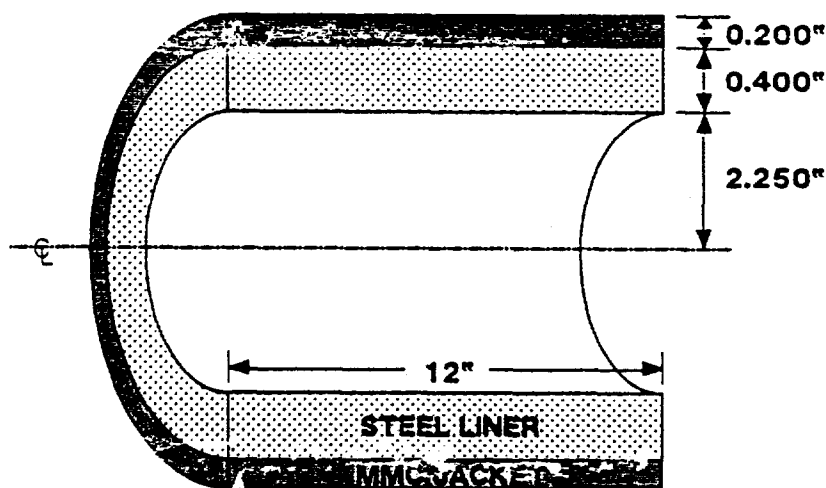


Figure 1. Jacketed cylinder geometry.

The cylinders were pressurized in increments over various pressure ranges before autofrettage, followed by hydraulic autofrettage and thermal soak operations. Table II gives the processing history of these cylinders.

TABLE II. CYLINDER PROCESSING HISTORY

Cylinder No.	3AE2	3AE5	3AA	3AN
Pressure history (Ksi)	14-33	14-33	16-35	16-35
Autofrettage pressure (Ksi)	37.1	37.1	38.6	39.3
Thermal soak (4 hrs)	700°F	600°F		

SPECIMEN PREPARATION

To measure the surface residual stress through the cross section normal to the cylinder axis, 1-inch thick rings were cut from the middle section of the cylinders. One sample each was obtained from 3AA and 3AN, and two were cut from 3AE, for a total of four rings. The rings were cut at Benet Laboratories on an Agie DEM315 travelling wire electrostatic discharge machine, which can produce strain-free samples with minimum mechanical and thermal damage. The ring surface was polished manually with sandpaper and then electropolished to remove surface effects due to sanding, machining, and oxidation. It was then washed with acetone, alcohol, and distilled water. The electropolishing setup was as follows:

anode	specimen to be polished
cathode	lead
solution	50% H ₃ PO ₄ (85% concentration) 25% H ₂ SO ₄ (98% concentration) 25% H ₂ O
current density	30 to 90 amp/dm ²
temperature	room
agitation	no external

CALIBRATION AND VERIFICATION PROCEDURE

A four-point bend experiment was formed to determine the elastic stress constant for the steel BCC 211 plane and to test the x-ray method. A 1-inch by 6-inch by 3/16-inch thick steel sample was used. An electrical strain gauge was applied to the specimen adjacent to where the x-ray measurements were made. Four-point bending generated tensile and compressive stresses between +100 Ksi and -100 Ksi. From the slope of the calibration curve, we determined the elastic modulus, E , to be 30.7 Msi (211.8 Gpa). The linear regression correlation coefficient was better than 0.95. To verify the x-ray method, four-point bend stress measurements using x-ray method versus strain gauge method are plotted in Figure 2. The agreement is very good, with a linear regression correlation coefficient of 0.97.

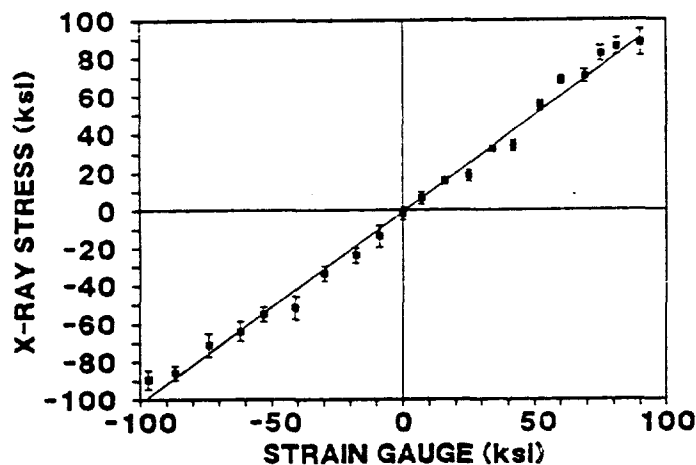


Figure 2. Four-point bend verification.

EXPERIMENTAL RESULTS

The hoop residual stress distributions in the steel liner as functions of the radial distance from the center of the cylinder are given in Figures 3 (3AE02), 4 (3AE05), 5 (3AA), and 6 (3AN). In these figures, each experimental point represents the average of five measurements taken at two-second intervals.

The error bars represent the dispersion in the measurements but do not include alignment, focusing errors, and effects due to surface irregularities. The solid curves are discussed later.

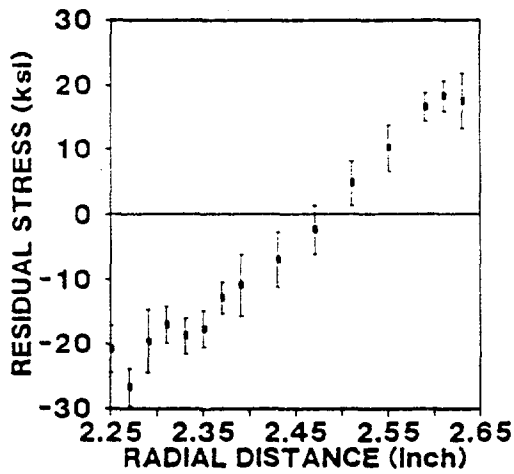


Figure 3. The measured 3AE02 hoop residual stress distribution.

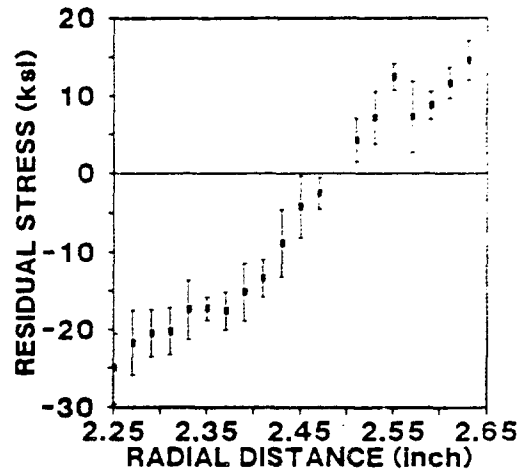


Figure 4. The measured 3AE05 hoop residual stress distribution.

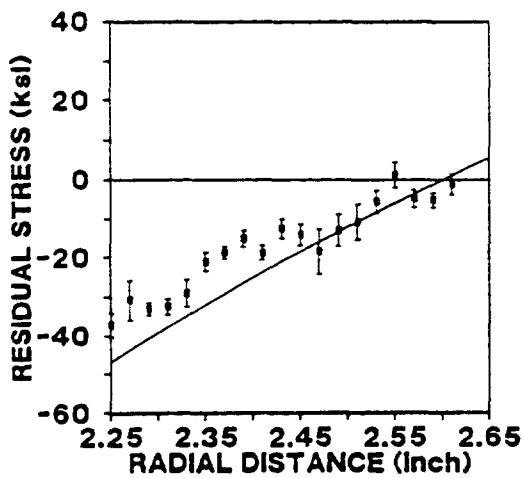


Figure 5. The measured 3AA hoop residual stress distribution with a line superimposed showing the predicted stress distribution.

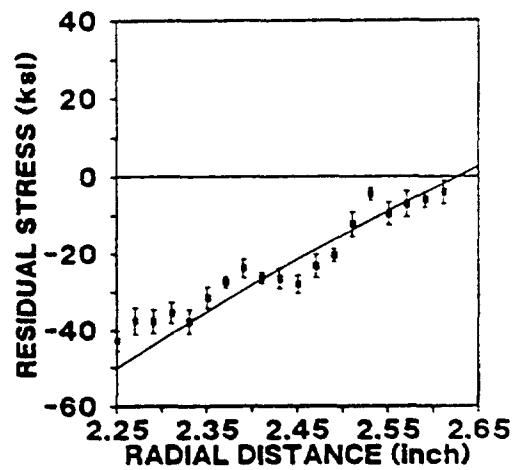


Figure 6. The measured 3AN hoop residual stress distribution with a line superimposed showing the predicted stress distribution.

It can be seen from our results that residual stress has been induced at the bore of the cylinders, diminishing and changing to tensile stress toward the outer edge of the steel liner. In cylinders 3AE02 and 3AE05, which were autofrettaged and thermal soaked, both compressive and tensile stresses were observed in the steel liner. In cylinders 3AA and 3AN, which were only autofrettaged, the residual stresses in the steel liner were mostly compressive. The characteristics of the distribution curves are similar to those for autofrettaged steel cylinders in the literature (ref 4).

Plots of strain versus $\sin^2\psi$ from the bore are given in Figure 7 (3AE05, 3AN), and plots of the steel/MMC interface are given in Figure 8 (3AE05, 3AN). From the slope of the $(D-DP)/DP$ versus $\sin^2\psi$ plot, where DP is the perpendicular spacing, compressive stresses at the bore are -17 Ksi (3AE05) and -35 Ksi (3AN), and tensile stresses at the interface are 14 Ksi (3AE05) and 0.5 Ksi (3AN). We used our previously-determined Young's modulus (30.7 Msi) for the steel 211 plane. The correlation coefficients for the linear regression fit for all the curves were better than 0.95 except the 3AN interface which was 0.46.

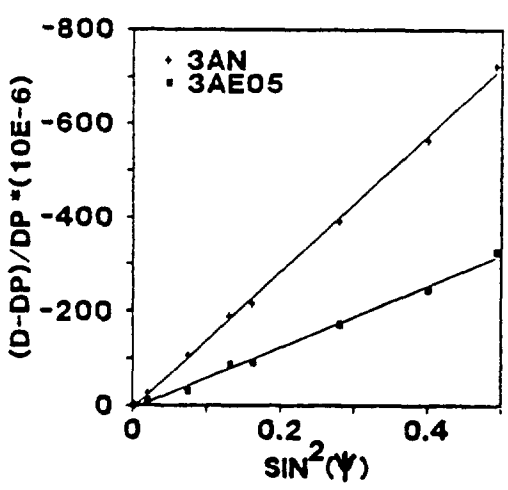


Figure 7. $\sin^2\psi$ determination of stresses at the cylinder bore.

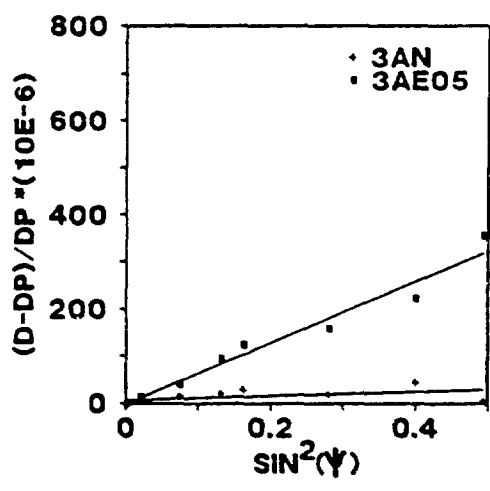


Figure 8. $\sin^2\psi$ determination of stresses at the interface.

The autofrettage pressure for cylinders 3AA and 3AN was 38.6 Ksi and 39.3 Ksi, respectively. Comparing Figures 5 and 6, compressive residual stresses 5 to 10 Ksi less were generated in 3AA than in 3AN. Comparing Figures 3 and 4 with Figure 6, compressive residual stresses approximately 15 to 20 Ksi less were generated in 3AE02 and 3AE05 than in 3AN. The theory in the next section predicts less compressive residual stresses for smaller autofrettage pressures. Moreover, less stress was observed in 3AE02 and 3AE05 than in 3AA and 3AN for the following reasons: (1) less autofrettage pressure in 3AE02 and 3AE05 (37.1 Ksi); (2) thermal relaxation in 3AE02 and 3AE05 causing residual stress relief (refs 5,6); and (3) possible gap formation between the liner and jacket due to the thermal process. No difference was observed in the residual stresses in 3AE02 and 3AE05, which were thermal soaked at 700°F and 600°F, respectively.

THEORETICAL CONSIDERATION

Figure 9 shows how the compound cylinder problem can be decomposed into two parts: (1) a steel cylinder with internal applied pressure p and a pressure q acting on the steel by the MMC, and (2) the MMC with a pressure q acting on the MMC by the steel cylinder. We compare our experimental results with two theoretical models.

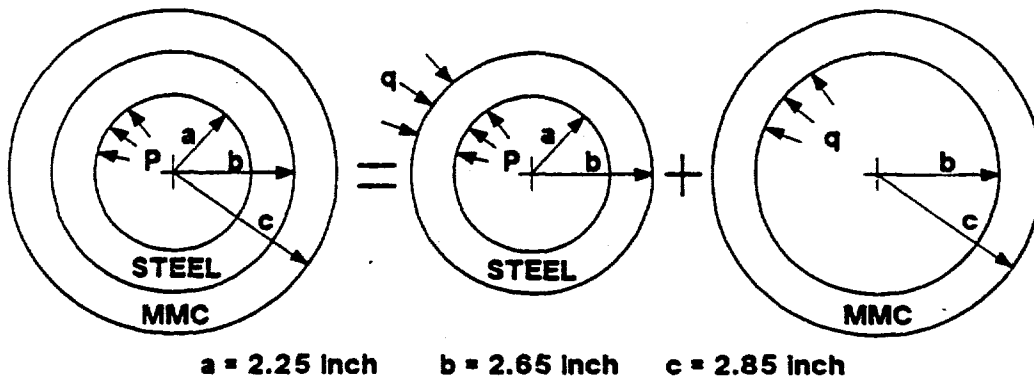


Figure 9. Decomposition of composite/steel cylinder.

The analytical predictions obtained from an elastic-plastic deformation autofrettage model (ref 7) are superimposed on the experimental distribution data in Figures 5 and 6. The calculations based on this model utilized the elastic constants in Table I and assumed the MMC was elastic. For the autofrettage pressure range of 37.1 Ksi to 39.7 Ksi, the steel cylinder can be considered fully plastic. Experimental results compared well with theoretical curves to within +10 Ksi.

The theoretical distribution of residual stresses based on Tresca's yield criterion was reported by Davidson et al. (ref 8). We obtained theoretical curves by assuming an all-steel monoblock 100 percent overstrain autofrettage model. In this model, the cylinders are considered fully plastic and the hoop residual stress distribution is given by

$$\sigma_t = \sigma_y \left(\frac{-\log w}{(w^2-1)} \left(1 + \frac{b^2}{r^2} \right) + \left(1 - \log \frac{b}{r} \right) \right) \quad (1)$$

where σ_t = hoop stress, σ_y = yield strength, $w = b/a$, and a, b, r = bore, outside, and variable radius, respectively.

Figure 10 gives the theoretical predictions based on this simple monoblock autofrettage model assuming: (1) the cylinder consists of the steel liner only and extends to a radius of 2.65 inches (top curve), and (2) the steel extends through the cylinder to a radius of 2.85 inches (bottom curve). We used 155 Ksi as the yield strength for steel. The experimental stress distribution results for cylinders 3AA and 3AE02 are superimposed on the analytical curves. The 3AE02 data points fall closely to the top monoblock curve, while the 3AA data points fall more closely to the lower monoblock curve.

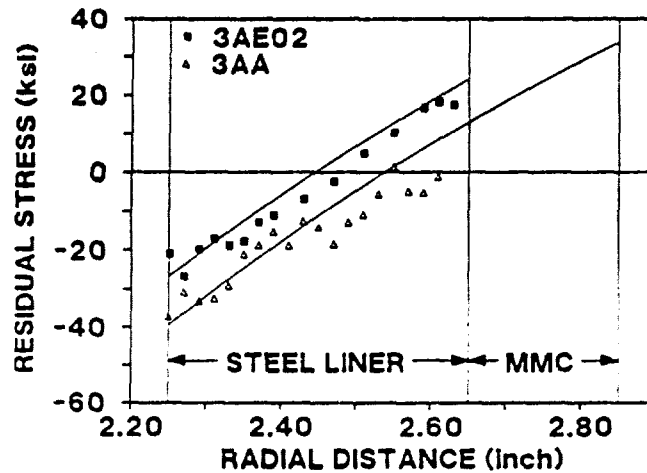


Figure 10. Monoblock plastic deformation calculations with 3AA and 3AE02 hoop residual stress distributions superimposed.

DISCUSSION

As indicated in Figure 10, in an all-steel plastic deformation autofrettage model, the compressive stress at the bore is balanced by the tensile stress at the outer part of the cylinder. A comparison of the zero crossings in our stress distribution curves indicates that in an MMC steel cylinder, tensile stress has been transferred into the MMC. From a consideration of the area under the stress curve in cylinders 3AE02 and 3AE05 (Figures 3 and 4), approximately 40 percent of the tensile residual stress has been transferred. In cylinders 3AA and 3AN (Figures 5 and 6), almost 100 percent of the tensile stress has been transferred into the MMC.

If we assume that the residual stress is approximately uniform, and the net compressive stress in the steel cylinder is balanced by the tensile stress in the MMC, then we can estimate the average tensile stress in the MMC cylinder. The results are as follows: 6 Ksi (3AE02, 3AE05), 30 Ksi (3AA), 42 Ksi (3AN).

In the autofrettage process, the bore is plastically enlarged and the MMC is elastically enlarged due to the internal hydraulic pressure. As this internal pressure is released, the outer MMC attempts to contract elastically to its

original dimension. The steel near the bore, which has been deformed the most, resists this action. This results in compressive hoop residual stress near the bore and changes to tensile stress near the outer surface. Since our 3AA and 3AN results compare favorably with theoretical predictions (ref 7), it appears that the model can be used to describe the autofrettaged compound cylinder.

In the thermal soak process, thermal stresses are added to the residual stresses and exceed the lower yield strength at elevated temperatures, permitting thermal relaxation in steel and aluminum. This causes the loss of bore expansion and compressive residual stresses in autofrettaged cylinders. The fact that 3AE02 was thermal soaked for 4 hours at 700°F, and the close comparison of 3AE02 data with the top monoblock curve in Figure 10, suggest a possible gap formation at the steel/MMC interface. If this occurs, the liner is dissociated from the jacket, and the monoblock model can adequately interpret the 3AE02 data. The effect of thermal relaxation on autofrettage in a compound cylinder should be investigated further both experimentally and theoretically.

REFERENCES

1. R.G. Hasenbein, E. Hyland, and G. Cunningham, "Laboratory Tests of Metal Matrix Composite-Jacketed Cylinders," ARCCB-TR-91016, Benet Laboratories, Watervliet, NY, April 1991.
2. C.O. Ruud, P.S. DiMascio, and D.J. Snoha, "A Miniature Instrument For Residual Stress Measurement," in: Advances in X-Ray Analysis, Plenum Press, New York, Vol. 27, 1984, p. 273.
3. S.L. Lee, M. Doxbeck, and G. Capsimalis, "Experimental Methods in Residual Stress Measurement Using a Position-Sensitive Scintillation Detection System," U.S. Army ARDEC Technical Report, Benet Laboratories, Watervliet, NY, to be published.
4. L. Pintschovius, E. Macherauch, and B. Scholtes, "Determination of Residual Stresses in Autofrettaged Steel Tubes by Neutron and X-Ray Diffraction," in: Residual Stresses in Science and Technology, Vol. 1, DGM Informationsgesellschaft mbH, Federal Republic of Germany, 1987, pp. 159-165.
5. V.C.D. Dawson and J.W. Jackson, "Investigation of the Relaxation of Residual Stresses in Autofrettaged Cylinders," Journal of Basic Engineering, March 1969.
6. J. Throop, J. Underwood, and G. Leger, "Thermal Relaxation in Autofrettaged Cylinders," in: Residual Stress and Stress Relaxation, (E. Kula and V. Weiss, eds.), Plenum Press, New York, 1982, p. 205.
7. P.C.T. Chen, "Elastic-Plastic Analysis of a Thick-Walled Composite Tube Subjected to Internal Pressure," ARCCB-TR-89027, Benet Laboratories, Watervliet, NY, October 1989.

8. T.E. Davidson, D.P. Kendall, and A.N. Reiner, "Residual Stresses in Thick-Walled Cylinders Resulting From Mechanically-Induced Overstrain," Experimental Mechanics, November 1963, pp. 253-262.

TECHNICAL REPORT INTERNAL DISTRIBUTION LIST

	<u>NO. OF COPIES</u>
CHIEF, DEVELOPMENT ENGINEERING DIVISION	
ATTN: SMCAR-CCB-DA	1
-DC	1
-DI	1
-DR	1
-DS (SYSTEMS)	1
CHIEF, ENGINEERING SUPPORT DIVISION	
ATTN: SMCAR-CCB-S	1
-SD	1
-SE	1
CHIEF, RESEARCH DIVISION	
ATTN: SMCAR-CCB-R	2
-RA	1
-RE	1
-RM	1
-RP	1
-RT	1
TECHNICAL LIBRARY	5
ATTN: SMCAR-CCB-TL	
TECHNICAL PUBLICATIONS & EDITING SECTION	3
ATTN: SMCAR-CCB-TL	
OPERATIONS DIRECTORATE	1
ATTN: SMCWV-ODP-P	
DIRECTOR, PROCUREMENT DIRECTORATE	1
ATTN: SMCWV-PP	
DIRECTOR, PRODUCT ASSURANCE DIRECTORATE	1
ATTN: SMCWV-QA	

NOTE: PLEASE NOTIFY DIRECTOR, BENET LABORATORIES, ATTN: SMCAR-CCB-TL, OF ANY ADDRESS CHANGES.

TECHNICAL REPORT EXTERNAL DISTRIBUTION LIST

	<u>NO. OF COPIES</u>		<u>NO. OF COPIES</u>
ASST SEC OF THE ARMY RESEARCH AND DEVELOPMENT ATTN: DEPT FOR SCI AND TECH THE PENTAGON WASHINGTON, D.C. 20310-0103	1	COMMANDER ROCK ISLAND ARSENAL ATTN: SMCRI-ENM ROCK ISLAND, IL 61299-5000	1
ADMINISTRATOR DEFENSE TECHNICAL INFO CENTER ATTN: DTIC-FDAC CAMERON STATION ALEXANDRIA, VA 22304-6145	12	DIRECTOR US ARMY INDUSTRIAL BASE ENGR ACTV ATTN: AMXIB-P ROCK ISLAND, IL 61299-7260	1
COMMANDER US ARMY ARDEC ATTN: SMCAR-AEE	1	COMMANDER US ARMY TANK-AUTMV R&D COMMAND ATTN: AMSTA-DDL (TECH LIB) WARREN, MI 48397-5000	1
SMCAR-AES, BLDG. 321	1	COMMANDER US MILITARY ACADEMY	1
SMCAR-AET-O, BLDG. 351N	1	ATTN: DEPARTMENT OF MECHANICS WEST POINT, NY 10996-1792	
SMCAR-CC	1		
SMCAR-CCP-A	1	US ARMY MISSILE COMMAND	
SMCAR-FSA	1	REDSTONE SCIENTIFIC INFO CTR	2
SMCAR-FSM-E	1	ATTN: DOCUMENTS SECT, BLDG. 4484 REDSTONE ARSENAL, AL 35898-5241	
SMCAR-FSS-D, BLDG. 94	1		
SMCAR-IMI-I (STINFO) BLDG. 59	2		
PICATINNY ARSENAL, NJ 07806-5000			
DIRECTOR US ARMY BALLISTIC RESEARCH LABORATORY ATTN: SLCBR-DD-T, BLDG. 305 ABERDEEN PROVING GROUND, MD 21005-5066	1	COMMANDER US ARMY FGN SCIENCE AND TECH CTR ATTN: DRXST-SD 220 7TH STREET, N.E. CHARLOTTESVILLE, VA 22901	1
DIRECTOR US ARMY MATERIEL SYSTEMS ANALYSIS ACTV ATTN: AMXSY-MP ABERDEEN PROVING GROUND, MD 21005-5071	1	COMMANDER US ARMY LABCOM MATERIALS TECHNOLOGY LAB ATTN: SLCMT-IML (TECH LIB) WATERTOWN, MA 02172-0001	2
COMMANDER HQ, AMCCOM ATTN: AMSMC-IMP-L ROCK ISLAND, IL 61299-6000	1		

NOTE: PLEASE NOTIFY COMMANDER, ARMAMENT RESEARCH, DEVELOPMENT, AND ENGINEERING CENTER, US ARMY AMCCOM, ATTN: BENET LABORATORIES, SMCAR-CCB-TL, WATERVLIET, NY 12189-4050, OF ANY ADDRESS CHANGES.

TECHNICAL REPORT EXTERNAL DISTRIBUTION LIST (CONT'D)

	<u>NO. OF COPIES</u>		<u>NO. OF COPIES</u>
COMMANDER US ARMY LABCOM, ISA ATTN: SLCIS-IM-TL 2800 POWDER MILL ROAD ADELPHI, MD 20783-1145	1	COMMANDER AIR FORCE ARMAMENT LABORATORY ATTN: AFATL/MN EGLIN AFB, FL 32542-5434	1
COMMANDER US ARMY RESEARCH OFFICE ATTN: CHIEF, IPO P.O. BOX 12211 RESEARCH TRIANGLE PARK, NC 27709-2211	1	COMMANDER AIR FORCE ARMAMENT LABORATORY ATTN: AFATL/MNF EGLIN AFB, FL 32542-5434	1
DIRECTOR US NAVAL RESEARCH LAB ATTN: MATERIALS SCI & TECH DIVISION CODE 26-27 (DOC LIB) WASHINGTON, D.C. 20375	1 1	MIAC/CINDAS PURDUE UNIVERSITY 2595 YEAGER ROAD WEST LAFAYETTE, IN 47905	1
DIRECTOR US ARMY BALLISTIC RESEARCH LABORATORY ATTN: SLCBR-IB-M (DR. BRUCE BURNS) ABERDEEN PROVING GROUND, MD 21005-5066	1		

NOTE: PLEASE NOTIFY COMMANDER, ARMAMENT RESEARCH, DEVELOPMENT, AND ENGINEERING CENTER, US ARMY AMCCOM, ATTN: BENET LABORATORIES, SMCAR-CCB-TL, WATERVLIET, NY 12189-4050, OF ANY ADDRESS CHANGES.